1. STATUS OF WIND TUNNEL WALL CORRECTION METHODS

Authors : C. Taylor } CHAPTERS 1.1 - 1.3
P. Ashill

A. Krynytzky } CHAPTER 1.4
J. Hackett

1.   STATUS OF WIND TUNNEL WALL CORRECTION METHODS

1.1   THE FUNDAMENTAL ASSUMPTION

In general, the aim of wind-tunnel tests is to make measurements of aerodynamic quantities under strictly controlled and defined conditions in such a way that, despite the presence of the tunnel walls, the data can be applied to unconstrained flow. The existence of a free-air flow which is "equivalent" to that in the tunnel is the fundamental assumption underlying the entire framework of the theory and practice of wind-tunnel wall constraint.

A rigorous definition of equivalence is complicated by the fact that wall interference varies over the model and its wake. If the wall interference were uniform, the equivalent free-air conditions could be defined quite simply as the values of Mach number, incidence and sideslip which, in free air, at the same total pressure and temperature, would give the same forces and moments as those measured in the tunnel.

The existence of spatial variations in the wall-induced velocities means that this equivalence cannot be obtained precisely and some corrections for these variations are needed. The standard approach adopted for tests of aircraft models, described below, is to correct the tunnel Mach number to the equivalent free-air value, and hence obtain the equivalent static and dynamic pressures. If these are used to obtain lift and sideforce coefficients, no further correction is needed, but the angles of incidence and sideslip do need correction. These corrections to Mach number and angles are referred to as "Primary Corrections". The residual variations in the wall-interference velocities can be interpreted as wall-induced distortions of the model and its wake and it is customary to make corrections for these, as discussed in Section 1.3. In most cases these corrections must be based on linearised theory of inviscid flow, as indeed are the corrections to the parameters defining the equivalent free-air flow.

Of course there are errors and uncertainties in the application of these corrections but, if these can be shown to be smaller than the required accuracy, the measured data are, by definition, correctable and the equivalent free-air principle is valid. If not, the data are correctable only to the accuracy determined by the uncertainty in the corrections and, if this is unacceptable, the data must be classified as uncorrectable, though not necessarily without value. The uncertainties in the corrections may be due to approximations in the correction formulae or to factors such as viscous-inviscid interactions in the flows over the model and at the tunnel walls, large model wakes or localised regions of transonic/supersonic flows, and, in general, they are difficult to quantify. The subject of correctability has been addressed by Kemp [12] who outlined a procedure for categorising the wall interference for each test data point and showed how, in principle, the tunnel geometry might be changed to enable correctable data to be obtained for a range of tests which might otherwise be classified as uncorrectable.
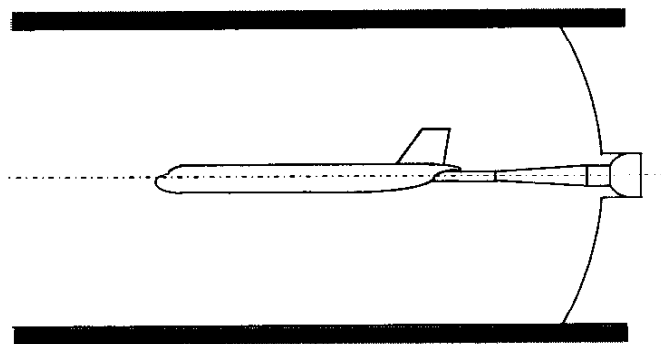
In practice, the issue is usually determined empirically by comparisons with nominally interference-free data, perhaps deduced from tests on models of different sizes or, more satisfactorily, by comparison with results of carefully-controlled experiments in adaptive-wall wind tunnels (Lewis and Goodyer [13], [14] and Ashill, Goodyer and Lewis [3]). Sometimes this can lead to the use of methods of wall correction that are at variance with the classical method outlined above (see, for example, Chapter 6 and Chapter 7) but the classical approach is the most commonly used for aircraft testing, particularly at cruise conditions, where experience suggests that it is valid.

A further element in the process of ensuring accuracy and consistency in the reduction of tunnel measurements to equivalent free-air values is the compatibility between the tunnel calibration and the correction procedure and this is addressed in Section 1.2.
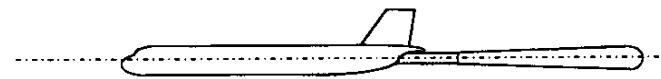
1.2 TUNNEL CALIBRATION AND BOOK-KEEPING OF CORRECTIONS.

Expressed in the most general terms the tunnel calibration establishes quantitative relationships between the flow conditions in the tunnel working section and reference measurements, made at positions in the tunnel which are sufficiently remote from the test volume for them to be unaffected by the presence of the model* . The flow conditions of primary interest are wind speed and direction and variations of these quantities over the space normally occupied by a model. Temperature profiles may also be measured.

The reference measurements which relate to wind speed are usually total and static pressure, together with total temperature and, although in principle, the calibration of the test section might be made using non-intrusive anemometry, it is normal practice to use a static-pressure probe and pressure-sensing yawmeters. Hence the calibration, which is intended to provide 'tunnel-empty' data as a reference base for corrections which allow for the constraining effects of the walls, may not do so unless account is taken of the presence of the probe in the application of constraint corrections.

One of two methods must be adopted:

a) the calibration data is corrected to a truly empty tunnel, or

b) the calibration data is not corrected for the wall-induced effects of the probe but, for wall constraint analysis, the flow displacement of the model and its sting support is reduced by that of the calibration probe.

a) Model on sting support

b) Definition of model

Figure 1.1   Method A

With the first approach (method A, Figure 1.1) the "model" must include the sting, terminated at an appropriate point upstream of the quadrant (Figure 1.1b), and the calibration data must be corrected to a tunnel configuration which is consistent with this. This means that the measurements of pressure on the probe should be corrected for the blockage of the probe, including its closure upstream of the quadrant (as shown for the model in Figure 1.1b) as well as for the direct effects of the nose and flare of the probe (i.e. their influence in unconstrained flow). If the method of constraint correction to be used is based on measurements of pressure changes at the tunnel walls, the wall pressure tappings must be included in the calibration and the datum measurements at these points should also be corrected for the direct and wall-induced effects of the probe.

This method, which is more suited to closed-wall tunnels, for which the corrections are easy to compute with the required accuracy, was adopted for the DRA 8x8 tunnel, and has been reported fully by Isaacs [11].

---

* This restriction does not apply to certain types of boundary-measurement methods which are 'autocorrective' in character. See Chapters 4.1 and 4.3.

If the second approach (method B, Figure 1.2) is adopted, the working section with the probe in place is defined as the empty tunnel (Figure 1.2b). When classical methods are used to calculate the model blockage, the appropriate source distribution should be that for the difference between the displacement flows of the model and the calibration probe, as shown in Figure 1.2c. This is also the case for methods of the one-variable type (see Section 4.1.1). The accurate use of a two-variable method (also defined in Section 4.1.1) will give the correct "model" displacement automatically, however this requires measurements of the differences in both streamwise velocity (or static pressure) and normal velocity at the boundary of the control surface.

Ideally, with method B, the downstream end of the calibration probe should have the same shape as the sting support for models, so that its displacement flow there is close to that for a sting-mounted model (the difference being that due to wake displacement). This limits the length of a "model" and, for ventilated tunnels, ensures that its displacement flow at the walls is mainly in that part of the working section which is likely to be unaffected by the re-entrant flows from the plenum at the down-stream end of the working section (e.g. at the re-entry flaps of slotted walls).

b) Empty tunnel

Model representation

EQUALS

MINUS

c) Definition of model

Figure 1.2   Method B

Figures 1.1 & 1.2 illustrate the case of sting-mounted models but similar arguments apply when the model is supported on struts i.e. either the struts can be taken as part of the model and the tunnel is calibrated empty or the tunnel is calibrated with the struts in place. Since the balance does not measure the loads on the struts the second approach is probably better but the correct choice may be influenced by the method used to account for strut interference. If this is determined experimentally, consistency must be maintained in the application of constraint corrections, both with the tunnel calibration and the basic test case. The same is true for tests to measure the support interference on sting-mounted models where particular care must be taken to avoid "double accounting" of wall interference associated with the sting.

If method B is adopted, tests of wall-mounted models would require a separate tunnel calibration. For this, either method could be used but, for method B, the probe would need to be wall-mounted from the same position as the model.
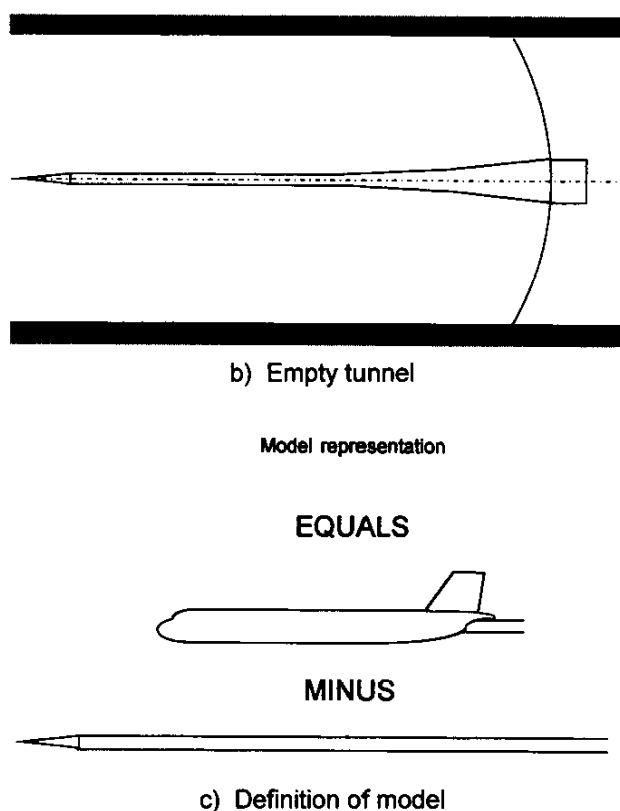
1.3 PRIMARY CORRECTIONS AND RESIDUAL VARIATIONS.

1.3.1 BASIC CONCEPTS.

Wall interference is never uniform and the variations over the model and its wake are often significant. There is therefore a choice to be made as to which values of the interference velocities should be used for making corrections. It is here that the concept of primary corrections and residual variations is applied and, as mentioned in Section 1.1, the primary corrections relate the tunnel test parameters to those of an equivalent free air flow.

During wind-tunnel experiments those test parameters which define the test conditions can be regarded as "primary"; basically these are total pressure and temperature, static pressure, together with model incidence and sideslip. These are the parameters to which primary corrections may be applied (normally no correction is needed for total pressure and temperature).

In most model tests the data reduction is made "on-line", using computerised systems. The usual procedure is to correct the measured tunnel reference static pressure to the equivalent free-stream static pressure. This entails using the tunnel calibration to obtain the appropriate "empty-tunnel" condition (as explained in section 1.2) and then to apply the correction for model blockage. The corrected tunnel static is then used to derive corrected Mach number (or velocity) and dynamic pressure, and these are used to compute values of force and moment coefficients. If the primary corrections are based on the proper choice of interference velocities no correction is needed to the measured, balance-axis, force-coefficients, which can then be used to compute the corrected angles of incidence and sideslip. These define the orientation of the free-stream flow vector and hence the directions in which the balance-axis forces should be resolved to obtain aerodynamic-axes forces.

The "residual variations" are the deviations from the freestream flow that is defined by the corrected primary test parameters. They can be thought of as wall-induced distortions of the model and its wake, and correcting the measurements for these distortions can present difficulties, particularly if the main interest is in the pressure distribution.

However, in tests of aircraft models, for which the forces and moments are determined by the Kutta condition at sharp trailing edges, corrections can be made for the effects of the variations of axial velocity and upwash on the measured forces and moments, see section 1.3.2. The difference between the wall-induced upwash at the tailplane and that at the wing is best treated as a change in tail setting.

When tests of models with wings of high aspect ratio are made at high tunnel pressure the aeroelastic distortion of the wing needs to be added to the wall-induced upwash in the determination of both the incidence correction and the residual variation. In cases where allowance has been made for aeroelastic distortion and upwash variation in the design of the model, so that the wing has a datum "effective" shape at a particular test condition, the corrections to incidence, and for residual variations, need to take account of this offset and its variation with tunnel pressure.

Although the bases for the incidence, moment and drag corrections can be derived rigorously for small perturbations in inviscid flow, as shown by Taylor [19], it must be realised that, in cases for which the effects of boundary and shear layers are dominant, this is only a first approximation and, in principle, the uncertainty in these corrections may be a factor in determining the accuracy of the test data. Also, in tests at high subsonic speeds, the residual variation in the streamwise velocity, for which no practicable

method of correction is known, may be a major cause for concern and this, along with the upwash variation, could limit the size of model which should be tested.

The maximum flow deviations that can be accepted will vary with the test objectives but Steinle and Stanewsky [20] have quantified a number of criteria for tests of aircraft-like models aspiring to the standards of high accuracy then current and, although these were formulated for "empty-tunnel" flows, it is logical to apply them to wall-induced variations also. As regards axial velocity, they proposed that the maximum allowable variation over the length of the model (streamwise gradient) should not exceed 0.06% of free-stream but in a later paper Bouis [7] suggested that, for subsonic testing, the maximum peak-to-peak variation in Mach number should be 0.001.

In this context it should be noted that Ashill, Taylor and Simmons [4] have shown that in closed-wall tunnels the effect of the model flow field on the wall boundary layers reduces both the blockage correction and the residual streamwise velocity variation. This effect, which is greater at the higher subsonic Mach numbers, is illustrated in Figure 1.3 (taken from that paper). This shows the residual variations in Mach number, relative to the correction applied at point 'A', for a wing-body model of a transport aircraft when tested in the 8ft closed-wall tunnel at DRA Bedford at a Mach number of 0.90. The contours obtained from calculations which include an allowance for the effect on the boundary layers on the tunnel walls of the wall pressure increments due to the presence of the model are shown in the right side of the Figure; those on the left are for inviscid flow at the walls. It can be seen that, at this high subsonic Mach number, the effect of the wall boundary layers is sufficient to reduce the residual variation over the wing from a value above Bouis' criterion to one which meets it. Although not specifically mentioned by Ashill et al, their calculations also showed that the thickening of the wall boundary layer, due to the presence of the model, was not sufficient to

Figure 1.3 Contours of constant residual blockage increment in Mach Number for transport aircraft model in DRA 8ft x 8ft Tunnel

give a significant axial pressure gradient. On the other hand, Hackett (1996) pointed out that gradient effects due to the growth of the wall boundary layers associated with large blockage models in low-speed tests are significant.

It can be expected that, in closed-wall tunnels, the interaction between the model flow field and the wall boundary layers will also reduce the variation in wall-induced upwash. This follows from the work of Adcock and Barnwell [1], who showed that the effects of the wall boundary layers are approximately the same as those of slotted walls. They derived a parameter defining the effective open-area ratio in terms of the thickness and shape parameter of the wall boundary-layer in the empty tunnel and, using the computational approach of Pindzola and Lo [16], gave charts showing the effects of the wall boundary layer on the interference parameters for small models. From these it can be inferred that, in tests of
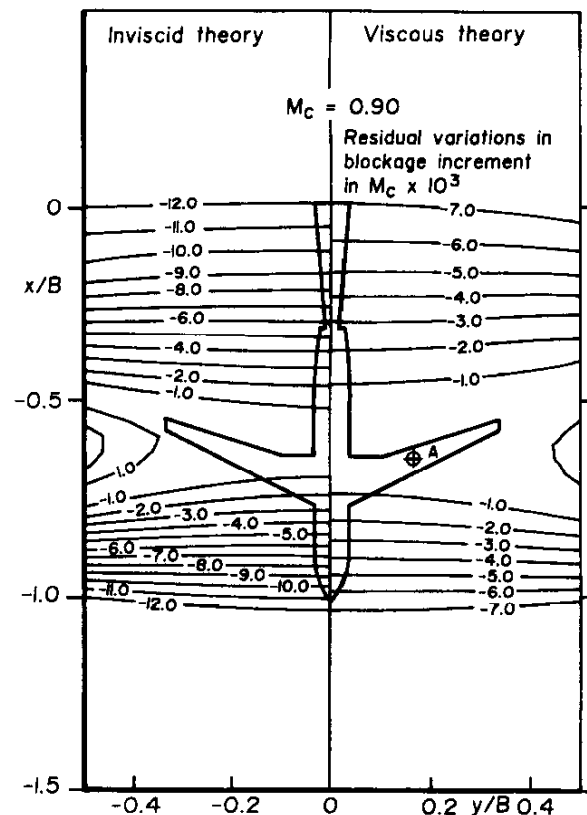
conventionally-sized models, the effect of wall boundary layers on the incidence correction at the model centre of pressure is likely to be negligible but that on the induced camber might be significant.

The calculation of primary corrections and residual variations can only be made when the boundary condition on the flow at the wall is formulated mathematically with sufficient accuracy. The calculations can be based on: a representation of the model (as in classical theory), measurements of pressures at the walls (see section 4) or on a combination of the two, although only the first and last of these may be suitable for "on-line" use.

For solid-wall wind tunnels, the wall boundary condition is well-defined and calculations can be made of wall-induced velocities using model representation methods (subject to allowance for wall boundary layers where necessary). Suitable methods are described in AGARDograph 109 and more recently Freestone of the Engineering Sciences Data Unit [8] has provided charts to allow calculations to be made of wall-induced upwash in solid-wall wind tunnels.

In ventilated tunnels, for which there is generally some uncertainty regarding the wall boundary condition, the primary corrections and residual variations cannot be calculated easily or accurately. Moreover the fact that a ventilated tunnel has low wall-interference (in the sense that the primary corrections are small) does not guarantee that this is also true for the residual variations. This is because all forms of ventilation have viscous losses at the wall and hence, to some degree, are like perforated walls, for which the interference velocities have significant gradients at the model. However the required data can sometimes be obtained experimentally, e.g. from careful comparison of test results with those for closed walls and, when obtained in this way, may be extrapolated to similar model configurations.

1.3.2   CORRECTIONS APPROPRIATE TO SPATIALLY-VARYING INTERFERENCE FLOWS.

AGARDograph 109 covers this topic and gives a number of formulae for aircraft-like models, in some cases offering a number of alternatives. Those for the corrections to angles and moments are based on the extrapolation of two-dimensional relationships and so, for wings of finite aspect ratio, are only approximate. Recently Taylor [19] has reviewed the subject and given formulae which, within the usual assumptions of the theory for small perturbations in subsonic inviscid flow, are exact. These cover the primary correction to incidence, and sideslip and the corrections for the residual variations. His results are given here, without proof, together with any restrictions on their validity which arise from flow conditions at the walls of the working section.

The corrections to incidence and pitching moment are derived from the application of a reverse-flow theorem. For two-dimensional flow, they have been investigated by Lewis and Goodyer [13], [14] and Ashill, Goodyer and Lewis [3], using an adaptive-wall tunnel. Their experiments covered a range of model incidence and Mach number, including cases where there were regions of supercritical flow on the upper surface of the airfoil and, in all instances, the data confirmed the validity of the linear-theory corrections. This suggests that the existence of supercritical flow on the upper surfaces of wings of finite span does not invalidate the results obtained from the theorem and hence they should be accurate for most tests of models at subsonic speeds.

1.3.2.1 PRIMARY CORRECTIONS.

The correction to incidence, at constant lift coefficient, is given by:

$$\delta\alpha = \frac{1}{S(dC_L / d\alpha)} \iint \bar{\ell}(1)w(x, y)dxdy,$$

where $\bar{\ell}(1)$ is the non-dimensional loading in reverse flow due to unit incidence and Uw(x,y) is the wall-induced upwash. In tests at high dynamic pressure there may be significant aeroelastic distortion of the wing, in which case this should be added to the wall-induced upwash.

In cases where the spanwise variation of the effective upwash is negligible and the chordwise variation is linear, the correction reduces to the simple expression:

$$\delta\alpha = w(\bar{x})$$

where $\bar{x}$ is the chordwise location of the aerodynamic centre in reverse flow. Hence for wings of infinite span, with a linear variation of upwash, the effective incidence is that at the 3/4 chord point, as originally suggested by Pistolesi [17], and, for slender wings with straight trailing edges, and attached flow at the leading edges, it is that at the trailing edge, as shown by Berndt [6].

Analogous expressions apply for the correction to angle of sideslip. In most cases there is little variation of sidewash over the tail fin and the correction to angle of sideslip, at constant sideforce, is then:

$$\delta\beta = v(\bar{x})$$

where $v(\bar{x})$ is the wall-induced sidewash at the position of the aerodynamic centre of the fin.

It is less clear which value of the velocity increment due to blockage should be used to correct the static pressure. Theory gives no guidance for most cases of practical interest and, intuitively, the best value is that which gives the least variation in blockage velocity over the most sensitive region of the flow. For aircraft models in tests at high subsonic speeds this is likely to be at the start of the recompression on the upper surface of the wing, but in cases for which the flow is dominated by a region of separation it is more likely to be that at the separation locus. There is some evidence (Ashill and Keating, [2] and Rueger and Crites, [18]) that the appropriate position for bluff-body flows with separation bubbles is where the blockage is a maximum.

1.3.2.2 Corrections for residual variations.

The corrections for residual variations include that for the variation of wall-induced streamwise velocity on profile drag and those for variations in wall-induced upwash (and aeroelastic distortion) on the lift-dependent drag and on the pitching and rolling moments of the wing. As noted above, the residual variation in sidewash over the fin is usually negligible and the effect of an axial variation in sidewash on the contribution of the body to the yawing moment, if significant, should be estimated by a method which allows for the effect of the boundary layer on the flow over the afterbody.

a)   Wall-induced pressure-gradient drag

Wall-induced pressure gradients affect drag in two ways:

- first, in an 'inviscid' way, that is without altering the development of the boundary layers and wake just downstream of the model (i.e. about 10 wake thicknesses), and

- second, in a viscous manner through changes in the development of the boundary layer on the model and of the wake near the model, resulting in changes in skin friction and boundary-layer form (or normal pressure) drag.

Classically, the second of these mechanisms is ignored. Thus, for slender, compact bodies typical of aircraft configurations (for which the virtual volume due to the effective acceleration of the flow may be ignored compared with the actual volume of the model), the contribution of the correction to normal pressure drag is written as:

$$\delta D = V dp \, / \, dx \tag{1.1}$$

where V is model volume and dp/dx is the streamwise pressure gradient due to wall interference.

The pressure-gradient term in equation (1.1) could be determined using boundary-measurement methods such as those reviewed in Chapter 4. If such methods are not available one could resort to classical methods as described in AGARDograph 109 and reviewed further in Chapter 2* . Using the latter approach, with the model represented by a doublet and the wake by a point source, Rogers in Chapter 5 of AGARDograph 109, showed that the correction to drag coefficient due to wall-induced pressure gradient in solid-wall wind tunnels may be written as:

$$\delta C_D = -(1 + 0.4M^2)C_D \varepsilon_S, \tag{1.2}$$

where C_D is the drag coefficient excluding the contribution of the trailing-vortex drag and ε_s is the non-dimensional increment in wall-induced streamwise velocity due to solid blockage. This correction is often referred to as the wake buoyancy correction, since it can be interpreted as resulting from the wall-induced pressure gradient due to wake blockage. Note that, while this result is based on the neglect of the second (viscous) effect mentioned above, the effect of viscosity enters the final expression (1.2) through the drag coefficient.

Taylor [19] considered the flow in wind tunnels with solid walls, idealised slotted walls and open jets. Using a different approach to Rogers, he applied the conservation equations (mass, momentum and energy) to the inviscid flow outside the displacement surface of the model and its shear layers. Ignoring the second (viscous) effect above and neglecting second order terms in the energy equation he obtained the result:

$$\delta D = (p_c - p_1)\Delta, \tag{1.3}$$

where p is static pressure, suffix c refers to the (primary) correction at the model reference position and suffix 1 to conditions far downstream of the model. Δ is the displacement area of the wake far downstream. Taylor noted that, for models with 'thin' wakes, the change in static pressure along the working section is small in magnitude compared with the blockage correction to pressure $\delta p = p_c - p_0$, where suffix 0 refers to conditions far upstream of the model. Therefore he replaced equation (1.3) with

$$\delta D = \delta p \Delta. \tag{1.4}$$

In tests of models with simulated engine flows, for which the definition of drag includes pre-entry and post exit components, the correction takes the form:

$$\delta D = \delta p(\delta A + \Delta),$$

---

* Results for wall-induced pressure gradients in perforated-wall wind tunnels of square cross section as a function of wall porosity can be found from graphs of 'wake blockage factor ratio' in the paper by Pindzola and Lo [16]. See also Chapter 3.

where δA is the change in cross-sectional area of the "engine flow" streamtube between stations far upstream and far downstream.

In the absence of powered engine-flow simulation $\delta A = 0$ and

$$\Delta = \frac{1}{2}(1 + 0.4M^2)SC_D,$$ (1.5)

where C_D is the drag coefficient excluding the contribution of the trailing-vortex drag. Thus combining equations (1.4) and (1.5) and noting that, to the order of approximation of linear theory,

$$\delta p = -\rho_0 U_0^2 \varepsilon.$$

it follows that

$$\delta C_D = -(1 + 0.4M^2)C_D \varepsilon.$$ (1.6)

Except for high-drag models the contribution of wake blockage to the term ε in equation (1.6) may be ignored to give

$$\delta C_D = -(1 + 0.4M^2)C_D \varepsilon_S$$

which is in agreement with the expression given by Rogers (equation (1.2)).

As observed by Taylor [19], methods for determining the corrections to drag using mass momentum and energy balance between far upstream and downstream, such as that of Taylor, and those given below for lift-dependent drag are only valid in tunnels for which:

a) the velocity perturbations at the walls, due to the model, do not induce a change in the drag of the walls which is comparable with the required data accuracy and

b) the tunnel working section is long enough for the perturbation pressures due to model lift and sideforce to be negligible at its ends.

The first condition excludes tunnels with perforated walls and for these there is no simple expression for the correction to profile drag which includes the effect of wall constraint on the wake. In this case, the only solution is to fall back on expressions such as equation (1.1).

Hackett [9] has questioned the validity of the classical model for solid-wall wind tunnels described in AGARDograph 109. He argued that the influence on the drag of the wake source (and its associated images) of the source/sink distribution representing the model is cancelled identically by the influence of the source/sink distribution (and its images) on the drag of the wake source. This leads to the result that the correction to drag for incompressible flow is:

$$\delta C_D = -C_D \varepsilon_w$$ (1.7)

where suffix w refers to the wake component of blockage. Further details of this kinematic approach may be found in Chapter 6.

Experience with tests on bluff models and models at high lift suggests that Hackett's flow model is preferable to the classical flow model. Recently, Mokry [15] has derived equation (1.6) from momentum considerations. However, he pointed out that the kinematic approach only allows for one of the effects of the walls on the wake streamwise momentum (due to the difference in streamwise velocity between the flow far upstream of the model and that far downstream outside of the wake) and does not include the

buoyancy effect. The latter would be expected to dominate for attached flows, whereas the evidence of Hackett's studies is that the volume-dependent buoyancy drag is much less important than the correction given by equation (1.6) for bluff models or high-lift models. Ashill and Taylor [5] have shown how it is possible to reconcile Mokry's analysis with the classical formula by allowing for the effect of the walls on the pressure drag of the displacement surface of the model and its shear layers. Hackett [10] has reiterated the reasons for preferring his result.

All these methods rely on inviscid models of the flow in that they do not allow explicitly for the effect on the development of the shear layers on and downstream of the model of the second (viscous) effect described above. This assumption appears justified for models with thin shear layers and attached flows. However, for flows on the point of separation or with regions of separation, the walls may influence the development of the model boundary layers and its wake. Thus consideration needs to be given to the theoretical simulation of real viscous flows in the wind tunnel or systematic wind-tunnel studies of the effect of tunnel walls on the model drag for there to be a complete understanding of this problem.

b) Lift-dependent drag

With these reservations, the correction to lift-dependent drag is determined by the change in the flow at the vortex sheet far downstream of the model, taking into account changes in the loading due to wall-induced upwash (and if necessary aeroelastic distortion of the wing). In general, the correction at zero lift can be ignored and then the correction to drag, at constant lift coefficient, becomes:

$$\delta C_D = C_L^2 \int \{\Gamma(y)\mu(y) - \Gamma'(y)\mu'(y)\}dy.$$

where $\Gamma(y)$ is the normalised spanwise loading on the wing due to unit lift coefficient and $\mu(y)$ is half the downwash induced by the infinite vortex sheet having the same spanwise distribution of vorticity as the wing at unit lift coefficient. The dashed symbols denote in-tunnel values. Here the functions μ and μ' can be regarded as spanwise weighting factors for induced drag.

If the spanwise loading is close to elliptic, and the span of the model (and the aeroelastic distortion) are not excessive, the effects of the change in loading will be small and the change in the weighting factor will be constant across the span. The drag correction is then given by Glauert's formula, i.e. $\delta C_D = \delta\mu C_L^2$, where $\delta\mu$ is simply the wall-induced downwash at infinity downstream.

Strictly this correction is a force directed along the tunnel axis, not along the corrected free-stream axis, but usually this distinction can be ignored and then the correction should be added to the drag force obtained by resolving balance-axis forces onto the corrected free-stream axis.

The difference between the correction given above and that obtained by simply multiplying the lift by the incidence correction, is due to the thrust force at the wing leading edge. As this force only occurs in fully-attached flow it might be expected that, when there is significant flow separation at the leading edge, the drag correction will be closer to the product of the lift force and the induced upwash at the model. This is obviously the case when the measured drag varies roughly as the product of lift and incidence, as for slender wings with sharp leading edges. When, as is often the case, the model is long compared with the height of the working section, there may be a significant wall-induced camber at high lift and since theory gives no guidance on the value of the upwash to use in either the incidence or drag correction, there must be a degree of uncertainty in the correct values for these.

c)   Pitching moment and yawing moment

The correction to pitching moment at constant lift, which again is derived using a reverse-flow theorem, is :

$$\delta C_m = -(1 / S)\iint \overline{m}(x_1)w(x, y)dxdy,$$

where $\overline{m}(x_1)$ is the loading in reverse flow due to a linearly-varying upwash $U(x-x_1)$, x_1 is the chordwise location of the moment reference axis and $\delta w(x,y)$ is the residual variation of wall-induced upwash (including model aeroelastic distortion).

When the spanwise variation of the residual variation is negligible and the chordwise gradient is linear, the correction becomes:

$$\delta C_m = -\lambda C_{mq}$$

where C_{mq} is the non-dimensional pitching moment derivative for (nose-up) rotation, about the spanwise axis passing through the aerodynamic centre in reverse flow and $\lambda = \overline{c}\, dw/dx$, with upwash $Uw(x)$.

As mentioned above, the difference between the wall-induced upwash at the tailplane and the correction to incidence is best treated as a change in tail setting.

The correction to the rolling moment of a yawed wing is analogous to that for pitching moment i.e.:

$$\delta C_\ell = -(1 / S)\iint \overline{\ell}(x, y)w(x, y)dxdy,$$

where $\overline{\ell}(x,y)$ is the loading in reverse flow due to unit rate of roll and $w(x,y)$ is the wall-induced upwash. In using this equation care needs to be taken that the correction has the correct sign.

When yaw is obtained by a combination of pitch and roll, as may be the case with sting-mounted models, the "upwash" terms in the corrections to incidence, pitching moment and rolling moment must be interpreted as the component of wall-induced velocity normal to the plane of the wing. A similar interpretation also needs to be made for "sidewash" in the correction to angle of yaw. In these cases there may be an additional component to the correction to rolling moment, to account for the change in load on the fin.

References for Sections 1.1, 1.2 and 1.3.

[1]   Adcock J.B. and Barnwell R.W. 1984, "Effects of boundary layers on solid walls in three-dimensional wind tunnels", AIAA Journal Vol 22, No 3.

[2]   Ashill, P.R. and Keating, R.F.A., 1988, "Calculation of tunnel wall interference from wall-pressure measurements." The Aeronautical Journal, Vol. 92, No. 911, pp. 36-53.

[3]   Ashill P.R., Goodyer M.J. and Lewis M.C. 1996, "An experimental investigation into the rationale of the application of wind tunnel wall corrections", ICAS-96-3.4.1, Sorrento, pp 798 - 808.

[4]   Ashill P.R., Taylor C.R. and Simmons M.J. 1995, "Blockage interference at high subsonic speeds in a solid-wall wind tunnel", Proceedings of PICAST 2-AAC 6, Vol 1, pp 81-88, Melbourne 20-23 March 1995.

[5]   Ashill P. R. and Taylor C. R., 1997, "A further contribution to the discussion on 'Tunnel-induced gradients and their effect on drag", Communicated to AIAA Journal., May 1997.

[6]   Berndt S.B. 1950, "Wind tunnel interference due to lift for delta wings of small aspect ratio", KTH Tech Note Aero TN 19.

[7]   Bouis X. 1984, "ETW Specification and its vindication", Document SC-ETW/D/27.

[8]   Freestone M. M., 1995, "Upwash interference for wings in solid-liner wind tunnels using subsonic linearised-theory", ESDU Data Item 95014.

[9]   Hackett J. E. 1996, "Tunnel-induced gradients and their effect on drag", AIAA Journal, Vol. 34, No. 12, pp 2725 - 2581.

[10]   Hackett J. E., 1997, "Reply to comments by Mokry and Ashill/Taylor on 'Tunnel-induced gradients and their effect on drag'", Communicated to AIAA Journal.

[11]   Isaacs D. 1967, "Calibration of the RAE 8ftx8ft wind tunnel at subsonic speeds, including a discussion of the corrections to the measured pressure distribution to allow for the direct and blockage effects due to the calibration probe", ARC R&M 2777.

[12]   Kemp W. B. Jr. 1976, "Towards the correctable-interference transonic wind tunnel", Proceedings of the AIAA 9th Aerodynamic Testing Conference, 7-9 June 1976, pp 31-38.

[13]   Lewis M.C. and Goodyer M.J., 1995, "Initial results of an experimental investigation into the general application of transonic wind tunnel wall corrections", Second Pacific International Conference on Aerospace Science & Technology, Sixth Australian Aeronautical Conference, Melbourne. Vol. 1, pp 71-80. 20-23 , March 1995.

[14]   Lewis M.C. and Goodyer M.J., 1996, " Further results of an investigation into general applications of wind tunnel wall corrections", Paper 96-0560, AIAA 34th Aerospace Sciences Meeting, Reno, January,.

[15]   Mokry M., 1997, "Comment on 'Tunnel-induced gradients and their effect on drag", Communicated to AIAA Journal., April 1997.

[16]   Pindzola M. and Lo C.F. 1969, "Boundary interference at subsonic speeds in wind tunnels with ventilated walls", AEDC-TR-69-47.

[17]   Pistolesi, E., 1933, "Considerazioni sul problema del bi-plane", Aeronautica, Rome 13, 185

[18]   Rueger, M., Crites, R. And Weirich, R., 1995, "Comparison of conventional and emerging ("measured variable") wall correction techniques for tactical aircraft in subsonic wind tunnels (invited paper) AIAA 95-0108, 1995.

[19]   Taylor C.R. 1996, "Some fundamental concepts in the theory of wind-tunnel wall constraint and its applications", DRA/AS/HWA/TR96055/1.

[20]   Steinle, F. and Stanewsky, E., Wind Tunnel Flow Quality and Data Accuracy Requirements, AGARD-AR-184, November 1982.

1.4 CHOICE OF CORRECTION METHOD
(A. Krynytzky & J. Hackett)

"Naturally the precision of calculated interference parameters is far greater than that of any experimental verification of the underlying theory." H. C. Garner, AGARDograph 109

Wall interference prediction, correction and, in some cases, minimisation for a given model and test environment are the objectives of any correction method. Section 1.3 has shown it is both useful and revealing to describe wall interference in terms of primary corrections and residual interference variations. The calculation of primary corrections for a spatially varying interference field (for subsonic inviscid flow) has been discussed, as well as a method for handling residual variations. The main outputs of any wall interference method are thus the primary corrections to freestream velocity (direction and magnitude). However, for large models and for Mach numbers in the high subsonic range, residual interference should be quantified as well. In the adaptive wall case for which the interference goal is zero by definition, residual interference is an appropriate measure of the quality of the adaptation. Intermediate outputs of an adaptive wall method are the wall settings to achieve minimum interference. Wind tunnel model data, corrected for the influence of the walls to equivalent free air conditions, represent the ultimate output of the application of a wall correction method.

The correctability of wind tunnel data to equivalent interference-free conditions may be rigorously evaluated by consideration of interference gradients for linear potential flows or by comparison of in-tunnel to unconstrained-stream flow solutions at corrected flow conditions (virtually mandatory for non-linear flows). Poor correspondence of results of the latter calculations implies a breakdown of the usefulness of wind tunnel test results: there is no interference-free flight condition that corresponds to the wind tunnel flow field in the vicinity of the model. This may occur if interference variations are great enough that simple corrections based on linear theory do not capture the actual integrated interference on the model. The difference in the flow field (in-tunnel to interference-free at nominal corrected conditions corresponding to the tunnel flow) may be due to strictly inviscid loading changes or, more insidiously, fundamental changes in the nature of the flow field around the model. These phenomena include changes in the boundary layer on the model with regard to either onset of separation or change in shock position for compressible flows, modification of separation bubble size or shape, or change in wake trajectory (viscous or vortex).

The choice of a correction method, or whether to bother with wall corrections at all, depends on required data precision and accuracy, and on available resources. Resources include instrumentation, computing hardware and software, qualified staff, and time.

In practice, one is often faced with sizing a model for a given set of test conditions. That is, given a test facility and test envelope, how large a model may be used to generate "valid" wind tunnel data? "Larger" is generally better from the standpoint of aerodynamic simulation for most applications (i.e., closest Reynolds number match, model geometric fidelity, or other model- to full-scale considerations). Permissible magnitudes of wall corrections depend on overall required data accuracies. An error analysis with target data accuracies should be done to establish target maximum levels of wall interference. Steinle and Stanewsky [17] derive permissible flow field variations for a variety of testing requirements. The parameters that relate most directly to wall interference are based on a drag accuracy requirement of 0.0001 ΔC_D (Table 1).

Item	Description	Value
M	Mach number accuracy	0.001
α, (w/U_∞)	Angle of attack (upwash) accuracy	0.01 deg (0.00017)
$[d(w/U_\infty)]/[d(x/c)]$	Flow curvature	≤ 0.03 deg
$[d(w/U_\infty)]/[d\eta]$	Spanwise flow variation	≤ 0.1 deg
$dM/[d(x/L)]$	Streamwise Mach gradient	≤ 0.0006

Table 1 Required Flow Field Accuracies Corresponding to $\Delta C_D = 0.0001$
(after Steinle and Stanewsky, [17])

These values provide benchmarks against which the accuracy of primary wall corrections and the spatial variation of the residual wall interference field can be tested. Since the magnitude of primary wall corrections may be small, uncertainties associated with their prediction may be as large as the corrections themselves. The evaluation of data uncertainty may need to take this into account. With a reasonable model size as a starting point, an iterative evaluation of wall interference balanced against accuracy and scaling needs will generate the data for an informed decision.

Four factors govern the aerodynamic interference of wind tunnel walls on a model:

1) Nature of the aerodynamic forces generated by the model, including not only lift, drag, and pitching moment, but also the constitution of the total drag (in classical terms, vortex, parasite, and separation drag) and the contributions of simulated power units (including rotors, propellers, fans, and jets).

2) Mach number

3) Size of the model relative to the dimensions of the test section (length, width, and height).

4) Type of test section walls.

1.4.1 MODEL AERODYNAMICS

Model aerodynamics refers to those aspects of the model that require explicit treatment or modelling in the evaluation of wall interference, exclusive of Mach number. These include the displacement (or volume) effect of the model and the customary aerodynamic forces: lift, drag, thrust, and pitching moment. These interference effects are well understood in an attached-flow context and are commonly addressed using classical wall interference concepts. However, the testing of models at high lift, with powered lift (e.g., rotors or lifting fans) can result in large vortex wake deflections within the tunnel that require special modelling attention. Separated wakes present another flow situation requiring additional modelling.

Together with Mach number and model size, model aerodynamics guides the complexity of model representation. For attached flows around small models at low Mach number, use of simple singularities of known strength is adequate (Chapter 2). More complex geometries or large models may require more accurate geometry representation as afforded by panel methods.

Separated wakes behind bluff bodies require special treatment, Chapter 6. In particular, wall pressure measurements can be used to advantage for this case in order to determine the appropriate representation of the separation bubble. Large lift forces may require consideration of wake deflections

in addition to accounting for the separated wakes often associated with configurations near maximum lift. Rotor testing at low speeds introduces additional complexity in that wake trajectories may result in fundamental changes of the in-tunnel flow relative to an interference-free flow. These flows associated with V/STOL configurations are discussed in Chapter 8. Unsteady interference effects largely have to do with cross-stream resonance within the test section walls (Chapter 9).

Boundary measurement methods discussed in Chapter 4 potentially provide advantages with respect to both model and wall representations. Chapter 10 outlines applications of these methods to adaptive wall tunnels, especially for tunnels with two flexible walls for both 2D and 3D testing. Two-variable boundary measurement methods provide the incontestable advantage of not requiring a representation of the model for determination of the interference. This feature is most useful whenever the exact nature of the aerodynamics at the model is not known: small supersonic flow regions near the model, large deflected wing wakes, or separated flow at the model. Though these methods are applicable to any tunnel, the most progress has been made for tunnels with closed walls, largely because of boundary measurement considerations. One-variable boundary measurement methods can be especially helpful for the case of ventilated walls, where sufficient uncertainty exists as to the proper wall boundary condition. Representation of the model is required for this approach.

The modelling of active power simulation (propellers, wind turbines, fans, turbo-powered simulators, blown nacelles or other jet simulation with at most small deflections of the propulsion streamtube) is typically approached by consideration of momentum-streamtube relationships and the use of appropriate source and sink singularities (Chapter 8).

1.4.2 Mach Number

Discussions of the AGARD Fluid Dynamics Panel Working Group 12 [1] used a classification of tunnel flows by speed range from the standpoint of adaptive wall tunnel operation. This classification serves well in a more general wind tunnel testing context because the flow physics are fundamentally the same in all wind tunnels. The first three speed ranges are of particular interest with regard to wall interference (see Chapter 10 for further discussion of these classifications):

1) Group 1: subsonic free stream, local embedded supersonic regions may occur near the model; region near the walls is well represented by linearised compressible flow equations.

2) Group 2: subsonic free stream; non-linear region (in unconfined flow) extends beyond the walls.

3) Group 3: near-sonic and supersonic free stream.

Group 1 flows permit the application of the linearised potential flow equation for the evaluation of wall interference. The effect of compressibility is linearised using the Prandtl-Glauert compressibility factor, $\beta = \sqrt{1 - M^2}$. The governing equation is linear and homogeneous, so that the principle of superposition applies. That is, the interference flow field can be considered an incremental flow field due to the wall potential that can be simply added to the flow due to the model potential. Because a wide variety of practical aerodynamic problems fall into this speed range, and because of the demonstrated success of linearised methods, most of the methods in this publication use the linearised potential equation (which after the Prandtl-Glauert transformation becomes Laplace's equation) as a starting point.

For Group 2 flow the non-linear portion of the flow field, strongest at the model, has grown to include a substantial, if not the entire, region between the model and the wall. In this case, the distortion of the compressible flow field around the model and at the wall location (relative to interference-free conditions)

requires the use of non-linear flow equations for proper characterisation. Wall interference is not easily characterised as an incremental flow field; the calculation of both the in-tunnel and interference-free flow fields may be required. Chapter 5 addresses the estimation of interference for these flows. Chapters 4 (boundary measurement methods) and 10 (adaptive walls) also include discussions of the use of non-linear governing equations. For cases with supersonic flow extending to the walls, the interference of the walls may include the effects of reflected compressible disturbances (compression and expansion waves) on the model. The appearance of reflected disturbances may be considered to be the threshold for classification in the next speed range.

Group 3 flow presents the most difficult situation from the standpoint of correctability in that the flow field between the model and the walls is fully supersonic. In a typical case, the flow around the model is dominated by multiple reflections of expansion and compression disturbances (originating at the model) from the walls, back to the model. Passive ventilated walls have successfully been configured to attenuate isolated shock waves, but a practical method for reducing nonplanar shock reflections for configurations of interest is yet to be demonstrated. An adaptive closed-wall approach to shock reflection attenuation has been demonstrated in 2D testing; the much more difficult 3D problem is beyond the grasp of the current state of the art.

As Mach number is increased into the supersonic range, a point is reached beyond which wall interference ceases to be an issue. This occurs when the flow disturbances from the model, consisting of compression and expansion waves that travel along characteristics, are reflected from the tunnel boundaries and pass downstream of the model. The flow field around the model is therefore interference-free. A first-order estimate of permissible model size in the supersonic speed range is made by simply calculating the Mach diamond based on the upstream Mach number from the model nose (or, if known, the position of the detached nose shock). Thus, for a model positioned at a distance z from the closest tunnel wall, the body length L should be less than $2 z / \tan \arcsin (1/M)$. For pointed bodies a more accurate calculation of shock wave trajectory is possible using the exact (Taylor-McColl) solution for conical flows.

For a given model and test section wall, a mapping of flow regimes provides guidance regarding wall interference requirements. A schematic of such a map in the Mach-C_L plane, Figure 1.4, shows the typical progression from Group 1 to Group 3 flow with increasing up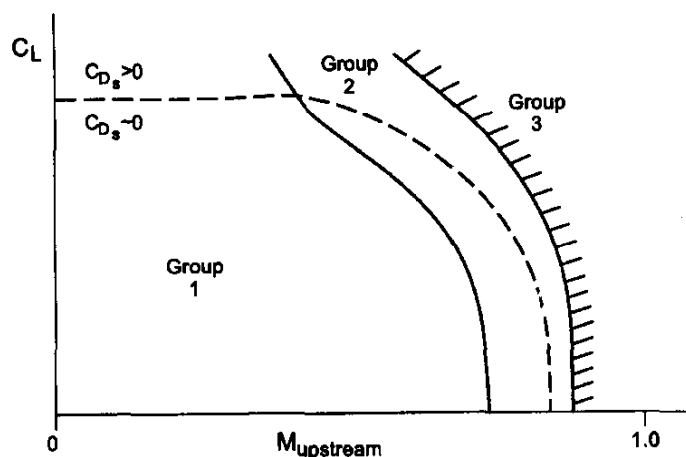stream Mach number at a given lift. With increasing lift the boundaries move to lower Mach numbers. Group 1 flows are amenable to linearised flow analysis. Group 2 flows will generally require non-linear flow analysis, and may not be easily correctable without resorting to an adaptive wall strategy. Group 3 flows are considered uncorrectable except for the case of fully adapted walls. Decreasing model scale (for a given configuration) will move the boundaries toward higher Mach number and lift. In this way, wall correction quality (for a given methodology) can be matched to desired test envelope by the appropriate choice of model size. It is recognised that the boundaries between flow

Figure 1.4 : Flow Regime Mapping for a Typical Subsonic Flight Vehicle

regimes are not distinct, but represent somewhat arbitrary transition zones between flow classifications. An additional boundary shown in Figure 1.4 delineates the onset of separation at the model. Interference estimates beyond this boundary should include an evaluation of separated wake interference.

1.4.3 MODEL SIZE

Model size relates to wall interference in two basic ways: (1) the gross dimensions of the model are directly proportional to the disturbances generated at the wall, and therefore to the magnitude of the interference felt by the model due to the walls, and (2) the physical extent of the model within the test section determines the severity of wall interference due to the spatial nonuniformity of the interference flow field. It should be noted that aerodynamic size of the model, which depends on the dominant flow phenomena and on the magnitude of the generated aerodynamic forces (see next section), rather than geometric size, is the most relevant characterisation of model size.

In classical wall interference theory (Chapters 2 and 3) models are first considered to be infinitesimal, so that any singularities representing the model's far-field disturbance may be considered to be located at a single point, with the primary interference velocity evaluated at that point and the resulting corrections applied. With regard to the magnitude of the disturbances due to the model, V (volume; for 2D flows, cross-sectional area A) and $C_D S$ (model drag; for 2D flows, C_d c) are taken to be the relevant linear scaling parameters representing the symmetric displacement of far-field streamlines, and $C_L S$ (model lift; for 2D flows, C_l c) for the asymmetric far-field perturbation due to the model. The strengths of the fundamental singularities used to represent the model are scaled by these model-dependent characteristics.

Model size, as relating to blockage interference, is often described or delimited by the so-called "model blockage" parameter, or A_{max}/C, where A_{max} is the maximum model cross-sectional area (taken normal to the tunnel axis), and C is the test section cross-sectional area. The 2D equivalent is t_{max}/H, where t_{max} is the maximum model thickness and H is the test section height. This parameter has an obvious geometric relationship to the afore-mentioned model volume (for 2D flows, area), depending on the model shape distribution. In the limit of 1D inviscid incompressible flow in a closed-wall tunnel, this area ratio is equal to the increase in effective freestream velocity at the model station. For compressible flow, in the limit of Mach approaching 1.0, this area ratio defines an upstream Mach number for which sonic choking in a closed-wall tunnel will most certainly occur. Thus, in these limiting cases, it is a physically meaningful parameter that bounds the parameters governing blockage interference. For normal model sizes the blockage interference is usually much less than predicted from 1D flow considerations (for example, for unusual shapes "when all is lost", Pope and Harper [14] suggest a factor of 1/4 to account for both solid and wake blockage, with A_{max} taken as the model frontal area). Finite model size and angle of attack contribute to the onset of sonic choking at a lower Mach number than predicted as above.

The first departure from point singularities considers the effect of finite span, both on the magnitude of the interference upwash at the centre of the model and on its spanwise variation. Similarly, model length may give rise to variations of interference from nose to tail, or root to tip for a swept wing. The relevant length scale for these effects are the cross dimensions of the tunnel, so that $2s/B$ (span ratio) and $L/\beta\sqrt{C}$ (body length ratio; for 2D flows, $c/\beta H$) form a logical nondimensionalised set of model dimensions for evaluating effects of the spatial variation of the interference field. In 3D subcritical flow, span and length ratios much less than 1.0 are adequately represented using point singularities at a single model location (as long as the model is either in the centre of the tunnel, or several model dimensions away from a homogeneous wall). This simple approach may prove adequate up to length ratios of one-half or more,

depending on required accuracy. Beyond about one-half, however, spatial nonuniformity of the interference field may become significant, so that multiple-singularity or panel methods should be used. In transonic flow, even very small models may experience unacceptable interference at Mach numbers close to one.

In general, the size of the aerodynamic perturbation due to the model at the wall location is a reasonable indicator of the magnitude of interference (for a given wall geometry). Within each speed range, moreover, there may be criteria for model size defining the validity of various wall interference approaches. This is most clearly demonstrated in the lowest speed range where linear potential flow applies. For linear subsonic flows, the model size criteria can be combined with Mach number using the Prandtl-Glauert factor β to scale physical model size for the first-order effects of compressibility. For example, for a given level of perturbation velocity at the wall, model volume should decrease like β^3.

1.4.4 WIND TUNNEL WALLS

Concurrent with advances in computational capability, significant developments have occurred with regard to wind tunnel wall geometry since the publication of AGARDograph 109 (Garner et al., [5]). In particular, with the rejuvenation of the adaptive wall concept (Sears, [16]), and subsequent boundary measurement methods, a variety of new approaches for the minimisation and evaluation of wall interference have been developed.

The type of wind tunnel walls spans a range of possibilities. With regard to wall interference methodologies, six approaches may be distinguished:

1) Closed parallel walls with no measurements at the boundaries (Chapters 2 and 6).

2) Closed parallel walls with boundary pressure measurements (Chapters 4 and 8).

3) Closed walls with deflection capability and boundary pressure measurements (Chapters 4 and 10).

4) Ventilated walls with no measurements at the boundaries (Chapter 3).

5) Ventilated walls with boundary measurements (Chapter 4).

6) Active ventilated walls with boundary measurements (Chapter 10).

The majority of existing wind tunnels have passive walls of basically fixed geometry, without adequate instrumentation at the walls for wall interference purposes. Closed-wall test sections of various cross sections are the most numerous for a variety of reasons: historical; relatively low power requirements for a given size and speed of the jet; unambiguous wall boundary condition and therefore well-understood interference characteristics; and potential for superior flow qualities (low spatial and temporal variations of pressure and velocity). Thus, advancements in adaptive wall technology notwithstanding, closed-wall tunnels with aerodynamically parallel walls (for a clear test section) are still the workhorses for most low-speed testing. For small models with attached flow, the use of classical methods (Chapter 2) generally suffices for the calculation of wall interference. Panel methods have proven to be successful extensions of classical techniques, particularly for the investigation of the wall interference of large models (Chapters 2 and 3).

For closed-wall tunnels, significant advances have been made in two areas since the publication of AGARDograph 109 [5]. First, with the development of boundary measurement techniques, the performance envelope of closed-wall tunnels has expanded to include larger models at low speed (both

from the standpoint of blockage and lift, Hackett, [7] and higher subsonic speeds for conventionally sized models (Ashill, Taylor, and Simmons, [4]). Boundary measurement techniques are discussed in Chapter 4 (Sec. 4.2 for closed walls) and adaptive walls, in Chapter 10. Second, the development of the adaptive-wall concept from both theoretical and practical standpoints (see Chapter 10 for a discussion of issues and approaches) has resulted in a deformable-wall test section being a serious candidate for new wind tunnel projects, especially for tunnels using a removable test section configuration.

In particular, practical implementations of the adaptive wall concept have resulted in a number of 2D test sections with deformable floor and ceiling. Theoretically, this is the simplest application of the adaptive wall concept. In principle, the design technology is little different from a flexible supersonic nozzle. Proper adaptation in three dimensions is a much more difficult problem, especially from the constructibility point of view. The rubber test section (Heddergott and Wedemeyer, [8]) and the octagonal deformable test section at the University of Berlin (Ganzer, Igeta, and Ziemann, [6]) are notable examples of deformable 3D closed-wall test sections. Difficulties associated with the desired arbitrary deformations have led to investigations of the use of 2D wall adaptation for 3D testing to minimise certain aspects of the interference (Wedemeyer [19]; Lamarche and Wedemeyer [10]; Wedemeyer and Lamarche [20]). Chapter 10 focuses on this approach as currently the most practical for providing wall interference reduction and control.

Ventilated wind tunnel walls have also undergone significant development in the past 30 years. Though the two basic types of ventilated walls, slotted and perforated, still predominate, a number of advances have been made in their use for the minimisation of wall interference. Experimental investigations of the ventilated wall boundary condition have met with mixed results: perforated walls behave like ideal porous walls over some range of crossflows, with possibly different inflow and outflow characteristics; walls with open slots exhibit a richness of behaviour only approximately captured by the ideal slotted-wall condition with the inclusion of porous-wall pressure-drop terms. Panel methods with the appropriate wall boundary conditions have been successfully applied to ventilated tunnel interference (Chapter 3). With the maturation of boundary measurement techniques, including the development of instrumentation and advances in data acquisition, the analytic forms of the wall boundary conditions can be side-stepped by applying the principles of the one-variable method (Chapter 4).

For perforated walls, a sliding perforated plate backing the primary perforated wall surface provides a means to vary wall openness. This type of wall configuration was pioneered at the Arnold Engineering Development Centre (AEDC) with slanted-hole walls, and is now a common feature of perforated wall retrofits, as well as of new designs. Initial experiments used the variable-porosity feature for global test section porosity variation to optimise clear test flow qualities and to minimise shock reflection at supersonic Mach numbers (Pindzola and Chew, [13]). However, it was realised that streamwise porosity variation could be used to minimise wall interference (Lo, [11]). To date, the TsAGI T-128 Transonic Wind Tunnel is the most ambitious implementation of this approach, the test section wall ventilation consisting of nominally 10% open normal holes, with 128 movable backing plates covering the entire test section (Neyland, [12]). The local porosity can thus be varied independently in each of the 128 zones from 0% (fully closed) to 10% (fully open). Successful adaptation is judged by comparing measured wall pressures to an interference-free prediction of far-field pressures. In general, perforated walls combined with wall pressure instrumentation provide an excellent opportunity for the application of measured boundary condition methods, (Sec. 4.3).

Operational adaptive features for slotted-wall wind tunnels have not yet evolved to the degree that perforated wall adaptation has. The importance of slot shaping has long been known to be important for supersonic flow forming in the low supersonic operating range (Ramaswamy and Cornette, [14]).

Research and development on the use of slot shaping to minimise wall interference has resulted in the calculation of particular slot shapes for minimum interference (Karlsson and Sedin, [9]; Agrell, Petterson, and Sedin, [2]). This work has resulted in a slot flow model that treats the re-entry flow from the plenum into the test section differently from the flow exiting the test section. The FFA T-1500 Transonic Wind Tunnel has manually replaceable contoured slot edges for each of the 16 longitudinal slots based on this work (Torngren, [18]). Various slot shapes were tested to optimise both clear tunnel flow qualities and wall interference. Though remotely actuated variable-geometry slot mechanisms have been proposed for several facilities, none has passed the proof-of-concept stage for wall interference minimisation. Investigations of the wall boundary condition for open slots suggest that the inclusion of a crossflow resistance term in the homogeneous boundary condition describes the actual crossflow boundary condition better than the ideal inviscid slot boundary condition. Real slotted tunnels thus appear to exhibit some of the interference characteristics of perforated-wall tunnels. These observations help bridge the apparent disparity in the fundamental forms of the ideal homogeneous slotted wall boundary condition and the ideal porous wall boundary condition.

A hybrid ventilated wall, consisting of longitudinal openings in the manner of slotted wind tunnels, but with fixed baffles within the slots that provide a D'Arcy-type resistance to crossflow, is used at the Ames 11-ft transonic leg of the Unitary Tunnel. As long as the slot spacing is small relative to the required absence of "graininess" of wall interference, this type of wall may be treated as a homogeneous perforated wall. With regard to shock reflection, Allen [3] shows that the strength of the reflected disturbance from a wall with lines of perforations changes little for more than five or six lines of perforations per wall. Open slots were found to have both a larger reflected disturbance than perforated walls and to require a larger number of slots (compared to lines of perforations) before the reflected disturbance approaches its asymptotic value. Other issues related to local wall non-uniformity include measurement locations and techniques for boundary measurement methods (Chapter 4), and supersonic shock wave cancellation.

An important length scale for these phenomena is the wall boundary layer thickness. It is expected that if the wall opening size and spacing are of the order of the boundary layer or less, then at many boundary layer thicknesses from the wall, the wall ventilation will be perceived as homogeneous. Similar scaling arguments apply to hole size and spacing for perforated walls. Since boundary layers in large wind tunnels are often several inches thick, permissible wall openness length scale may be of this order. Perforated wall openings and spacings are typically less; slot widths may be somewhat larger; but slot spacings are often an order of magnitude greater. The small size of wall openings for perforated wall tunnels and the consequent ability to attenuate impinging shocks and expansions explains their being preferred over slotted walls for low supersonic testing. These general considerations suggest that homogeneous modelling of ventilated walls is appropriate for typical wall configurations, with the notable exception of walls with only several open slots. The non-trivial aspect of this modelling is the value of the crossflow coefficients in the boundary condition. The inclusion of wall boundary layer effects on crossflow characteristics has been investigated, but the uncertainty associated with the estimation of the wall boundary layer on a ventilated wall for a variety of model test conditions presents great difficulty for practical use of this approach. These considerations favour boundary measurement methods for ventilated walls to provide the necessary boundary condition information. For closed-wall tunnels, these methods have also been found to implicitly account for at least part of the effect of the model on the wall boundary layer (see Sec. 4.2).

The test section downstream of the model is an area that gives rise to special problems relating to the interference and modelling of wind tunnel test environments. Difficulties in this area can be attributed to support interference and re-entry/diffuser flow. It is becoming increasingly apparent that careful modelling of these aspects of the test environment is required to evaluate interference in its entirety.

The use of advanced methods is recommended whenever simpler methods fail to satisfy accuracy requirements, which can occur under a variety of conditions:

1) Model is not small.

2) Large regions of separated flow dominate the flow field due to the model.

3) Large regions of supersonic flow exist around the model.

4) Supersonic flow extends to any wall surface.

5) Pressure perturbations at the wall are large enough to effect changes in the wall boundary layer thickness.

6) Streamline deflection due to model-generated forces is significantly modified relative to interference-free conditions.

Advanced methods can (and should) be used whenever they are available (subject to resource constraints), providing that their application for simple attached-flow cases has been validated. Conscientious scrutiny of wall interference results for a range of model geometries and flow conditions can provide valuable clues relative to improved implementations of wall interference methods for specific facilities.

In spite of several decades of research activities aimed at the development of superior wind tunnel wall configurations, no single type of wall has emerged as dominant for 3D testing in the subsonic and transonic speed ranges. Production and research testing facilities around the world now exhibit a wider variety of wall types than ever before. In most cases, testing organisations have large capital and infrastructure investments in their test facilities. Development efforts often target extending the performance envelope (at minimum cost) or understanding the peculiarities of each facility. Wall interference activities are thus proceeding on several fronts, some of which overlap, others which are mutually exclusive. Chapter 12 summarises areas where progress is both needed and anticipated to improve the understanding, evaluation, and control of wind tunnel wall interference.

REFERENCES FOR SECTION 1.4

[1]   AGARD Fluid Dynamics Panel Working Group 12, *Adaptive Wind Tunnel Walls: Technology and Applications*, AGARD-AR-269, April 1990.

[2]   Agrell, N., Petterson, B., and Sedin, Y. C-J., "Numerical Design Parameter Study for Slotted Walls in Transonic Wind Tunnels", ICAS-86-1.6.2, 1986.

[3]   Allen, H. J., "Transonic Wind Tunnel Development of the National Advisory Committee for Aeronautics", AG 17/P7, 6th Meeting of the Wind Tunnel and Model Testing Panel, November 1954.

[4]   Ashill, P. R., Taylor, C. R., and Simmons, M. J., "Blockage Interference at High Subsonic Speeds in a Solid-Wall Tunnel", *Proceedings of PICAST2-AAC*, Vol. 1, Melbourne, 20-23 March 1995.

[5]   Garner, H. C., Rogers, E. W. E., Acum, W. E. A., and Maskell, E. C., *Subsonic Wind Tunnel Wall Corrections*, AGARDograph 109, October 1966.

[6]   Ganzer, U., Igeta, Y., and Ziemann, J., "Design and Operation of TU-Berlin Wind Tunnel with Adaptable Walls", ICAS-84-2.1.1, 1984.

[7]   Hackett, J. E., "Living with Solid-Walled Wind Tunnels", AIAA-82-0583, March 1982.

[8]   Heddergott, A. and Wedemeyer, E., "Some new test results in the adaptive rubber tube test section of DFVLR Gottingen", ICAS-88-3.8.1, 1988.

[9]   Karlsson, K. R. and Sedin, Y. C.-J., "Numerical Design and Analysis of Optimal Slot Shapes for Transonic Test Sections - Axisymmetric Flows", AIAA-80-0155, January 1980.

[10]   Lamarche, L. and Wedemeyer, E., "Minimisation of Wall Interference for Three-Dimensional Models with Two-Dimensional Wall Adaptation", VKI-TN-149, March 1984.

[11]   Lo, C.-F., "Wind-Tunnel Wall Interference Reduction by Streamwise Porosity Distribution", Technical Note, AIAA Journal, Vol. 10, No. 4, April 1972.

[12]   Neyland, V. J., "Review of TsAGI Wind Tunnels", Proceedings of the International Conference on Wind Tunnels and Wind Tunnel Test Techniques, Southampton, UK, September 1992.

[13]   Pindzola, M. and Chew, W. L., "A Summary of Perforated Wall Wind Tunnel Studies at the Arnold Engineering Development Centre", AEDC-TR-60-9, August 1960.

[14]   Pope, A. and Harper, J. J., Low Speed Wind Tunnel Testing, John Wiley & Sons, Inc., New York, 1966.

[15]   Ramaswamy, M. A. and Cornette, E. S., "Supersonic Flow Development in Slotted Wall Wind Tunnels", AIAA 80-0443, 1980.

[16]   Sears, W. R., Self-Correcting Wind Tunnels, Aeronautical Journal, February/March 1974.

[17]   Steinle, F. and Stanewsky, E., Wind Tunnel Flow Quality and Data Accuracy Requirements, AGARD-AR-184, November 1982.

[18]   Torngren, L., "The FFA T1500 Injection Driven Transonic Wind Tunnel", ICAS-90-6.2.3, 1990.

[19]   Wedemeyer, E., "Wind Tunnel Testing of Three-Dimensional Models in Wind Tunnels with Two Adaptive Walls", VKI-TN-147, October 1982.

[20]   Wedemeyer, E., and Lamarche , L., "The Use of 2-D Adaptive Wall Test Sections for 3-D Flows", AIAA-88-2041, AiAA 15th Aerodynamic Testing Conference, San Diego, CA, May 1988.